Ge/Si quantum dots thin film solar cells

Zhi Liu, Tianwei Zhou, Leliang Li, Yuhua Zuo, Chao He, Chuanbo Li, Chunlai Xue, Buwen Cheng,[a] and Qiming Wang
State Key Laboratory on Integrated Optoelectronics, Institute of Semiconductors, Chinese Academy of Sciences, Beijing 100083, People's Republic of China

(Received 7 May 2013; accepted 4 August 2013; published online 19 August 2013)

Thin film *p-i-n* solar cells (SCs) with 30 bilayers undoped or p-type self-assembled Ge/Si quantum dots (QDs) were fabricated on n^+-Si(001) substrates by ultrahigh vacuum chemical vapor deposition. Compared with the SCs without Ge QDs, the external quantum efficiency in infrared region and the short-circuit current densities of the SCs with Ge QDs increased. However, their open-circuit voltages and efficiencies decreased. The open circuit voltages of p-type Ge/Si QDs SCs recovered significantly at low temperature, which was due to the suppression of recombination centers and longer carrier lifetime. © *2013 AIP Publishing LLC*. [http://dx.doi.org/10.1063/1.4818999]

Single crystalline solar cells (SCs) have been important research topics for decades, because of their stable characteristics and good power conversion efficiency. However, the bandgap nature of the material results in wasted photon energy below the bandgap.[1] Many researchers have conducted studies to enhance the performance of SCs by efficiently absorbing the sub-band-gap light. Recently, SCs using quantum dots (QDs), which enable the optical absorption of photons with energies below the band gap of the host have attracted many attentions.[2] Many InAs/GaAs system QDs SCs have been reported to be highly efficient SCs.[3–7] Although the increased short-circuit current density (I_{SC}) has been reported in SCs with QDs, the recombination centers and defects of the QD/bulk interface introduced by QDs,[6,8] all the reported experimental open-circuit voltage (V_{OC}) and efficiencies of QD SCs are less than those of optimum single-junction devices. However, the recombination in QDs also depends on the potential barriers and band alignment of QDs.[9] In Ge/Si QDs, a type II band offset is formed in which electrons and holes are spatially separated by heterostructures, and holes are confined in the Ge QDs.[10] Owing to the indirect band gap nature of Si and Ge and the type II band alignment in Ge/Si QDs, Ge QDs should exhibit a long carrier lifetime.[10,11] This alignment and the choice of a suitable thickness for the Si spacer layer allow the vertical transport of charge carriers between densely stacked Ge QDs, which enhances the photocurrent and minimizes the recombination of electrons and holes within Ge QD.[12,13] Thus, Ge/Si QDs are possibly a better material choice for QDs SCs. Many studies have concentrated on the photovoltaic characterizations of undoped Ge/Si QDs SCs.[9,11,14–16] However, considering to half-fill the Ge/Si QD levels and enhance the inter-level optical transitions between localized hole states, p-type doping is necessarily.[5,17–19]

In this work, SCs were fabricated using 30 bilayers undoped or p-type Ge/Si QDs structure on Si substrates. Photoluminescence (PL), external quantum efficiency (EQE), and conversion efficiency under illumination of SCs were determined at room temperature. Temperature-dependent V_{OC} was studied. A significant voltage recovery of SCs with Ge QDs was observed.

The samples were grown by cold-wall ultrahigh vacuum chemical vapor deposition (UHV-CVD) on n^+-Si(001) substrates with a resistivity of 0.001 Ω cm, using pure disilane (Si_2H_6) and germane (GeH_4). The Si substrates were first cleaned using an *ex situ* improved RCA wet-chemical cleaning recipe, and then loaded into the pre-treatment chamber. Before growing, the substrate was degassed at 300 °C in the pre-treatment chamber and heated to 920 °C for 5 min in the growth chamber with a background pressure lower than 1×10^{-7} Pa to deoxidize. Then, a 120 nm thick undoped Si buffer layer was grown at 750 °C with a flow of 6 sccm pure Si_2H_6 to obtain a flat starting surface. After a 240 s growth interruption to change growth temperature, seven undoped monolayers (MLs, 1 ML = 6.27×10^{14} Ge atom cm^{-2}) of Ge was deposited at 580 °C with a rate of 0.056 Å/s. The gas flow rate was 2 sccm pure GeH_4 with growth pressure of about 10^{-3} Pa. After a short growth interruption, 21 nm of undoped or lightly boron-doped (supplied by diluted B_2H_6) Si space was deposited at 580 °C, at a flow of 6 sccm pure Si_2H_6 with growth pressure of about 5×10^{-2} Pa. The boron doping concentration was about 5×10^{17} cm^{-3}. After a third growth interruption, the remaining 29 bilayers were grown in the same way. Each bilayer contained 7 MLs Ge and 21 nm Si space. A 120 nm undoped Si blocking layer and a 240 nm Si top contact layer with boron doping of 1×10^{19} cm^{-3} were deposited at 580 °C. Samples were grown below 600 °C (except the Si buffer layer) to prevent Si-Ge interdiffusion.[20,21] The sample with 30 layers of 21 nm undoped Si layers (without Ge QDs) was also grown in the same conditions. Thus, the only difference between the samples was the presence of Ge QDs. The reflection high energy electron diffraction system was used to *in situ* monitor the growth of Ge QDs and Si spacers.

Rectangular mesas with area of 0.016 cm^2 was fabricated by dry etching 1.3 μm down to the n^+-Si(001) substrate using an inductively coupled plasma etcher. After a 900 nm thick SiO_2 film was deposited, metal contacts were formed with a 100 nm Ni adhesion layer and a 900/50/50 nm thick Al/Ti/Au layer. The cross-sectional view of the device is shown in Fig. 1(a). Three kinds of SCs were marked as

[a]Author to whom correspondence should be addressed. Electronic mail: cbw@semi.ac.cn. Tel.: +861082304762.

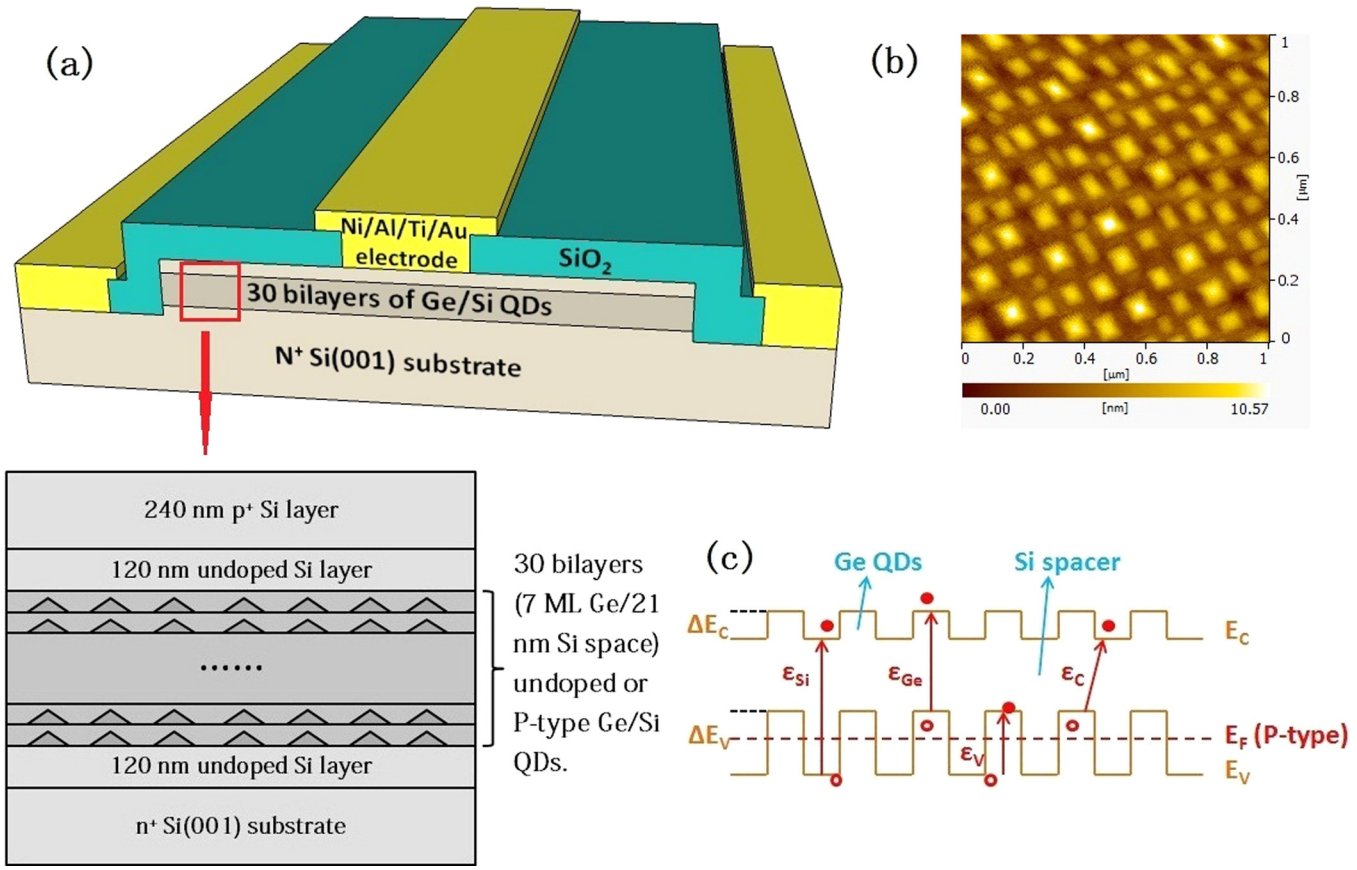

FIG. 1. (a) Cross-sectional view of the SCs with Ge QDs. Each bilayer contains 7 ML Ge and 21 nm Si space. (b) A 1 μm × 1 μm AFM image of the Ge/Si QDs. (c) Band edge diagrams of multilayer Ge/Si QDs. E_C, E_V, and E_F are the conduction band edge, the valence band edge, and the Fermi level (p-type) of multilayer Ge/Si QDs, respectively. Four common types of band transitions in multilayer Ge/Si QDs are shown.

SCs-A, SCs-B, and SCs-C, which corresponded to SCs without Ge QDs, SCs with undoped Ge QDs, and SCs with p-type Ge QDs, respectively.

To study the morphology of Ge QDs, four bilayers Ge/Si QDs sample with top Ge QDs without cover Si cap was deposited. The shape and morphology of the Ge QDs were examined by atomic force microscope (AFM). Fig. 1(b) shows a 1 μm × 1 μm AFM image of the Ge QDs. The morphology of the sample was dominated by small pyramidal Ge QDs. The average size of Ge QDs was about 60 nm × 5 nm (base width × height). The area density was about 2×10^{10} cm^{-2}.

A simplified type II band edge diagram of multilayer Ge/Si QDs is shown in Fig. 1(c). Four common types of band transitions exist in multilayer Ge/Si QDs. Here, ε_{Si} is the absorption edge of bulk Si, ε_{Ge} is the transition energy between valence band and conduction band of Ge QDs, ε_C is the phononless transition between valence band of Ge QDs and conduction band of Si,[10] and ε_v is the transition energy between the valence bands of Si and Ge QDs. Here, ε_{Ge}, ε_C, and ε_v were dependent on the Ge content and size of the Ge QDs.[22] To obtain the accurate band edge of Ge/Si QDs SCs, room temperature PL spectra of the sample with 30 bilayers Ge/Si QDs was performed. PL measurements were performed with LabRam HR 800 Raman instrumentation with InGaAs photodetector within the 1000 nm to 1600 nm range at room temperature using a 488 nm line of Ar^+ laser with a power of 10 mW (Fig. 2(a)). The PL spectra consisted of a broad peak from 1250 nm to 1600 nm and a shortwave shoulder around 1150 nm. The PL decreased around 1460 nm, which was induced by the color filter of the instrumentation. The broad peaks were attributed to the emission of Ge QDs,[23,24] which indicates the potential absorption levels or band of multilayer Ge QDs in the infrared region. The shortwave shoulder was attributed to the emission of the Si bandgap.

EQE was measured using tungsten and xenon lamps as light sources that pass through a monochromator. The EQE of three SCs are shown in Fig. 2(b). The resonance fringes in EQE were caused by the Fabry–Pérot cavity created by the SiO_2/Si and SiO_2/air mirrors. Compared to SCs-A, an appreciable infrared absorption enhancement from 900 nm to 1500 nm for SCs-B or SCs-C was observed. This phenomenon agrees with a previous report of SCs with Ge QDs.[16] From 600 nm to 900 nm, SCs-B and SCs-C also exhibited the absorption enhancement. The absorption enhancement from 600 nm to 900 nm was due to the increase absorption coefficient induced by Ge QDs. The difference between EQE of SCs-B and SCs-C was attributed to the higher barrier around undoped Ge QDs, which could blocks the photocarrier transfer.[25]

The current-voltage (I-V) characteristics of the devices in the dark and under illumination (a standard solar simulator) were obtained using a Keithley 4200 semiconductor characterization system. The I–V characteristics of the three SCs under standard illumination at room temperature are

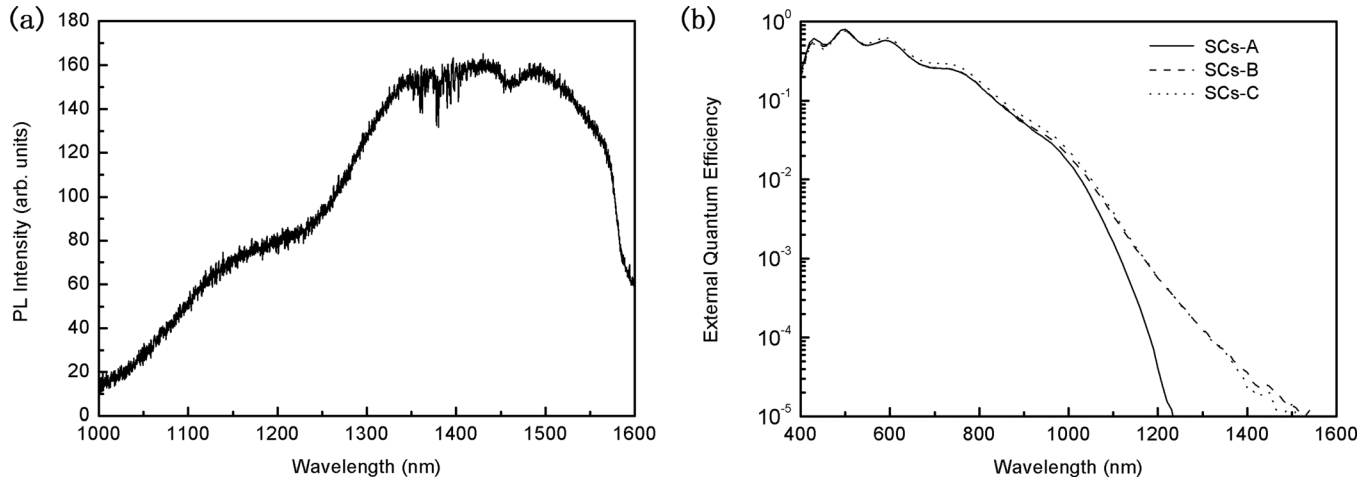

FIG. 2. (a) Room temperature PL spectra of Ge/Si QDs. (b) The EQE of the three SCs. Compared with SCs-A, EQE in the infrared region up to 1500 nm was observed for SCs-B and SCs-C.

shown in Fig. 3. The I_{SC} values of the SCs with Ge QDs were larger than those of the SCs without Ge QDs, which agrees with the EQE of the SCs. SCs-C had the largest I_{SC}, but its V_{OC} and fill factor (FF) were the lowest, which was due to the higher defect density induced by doping.[23,26] This phenomenon was confirmed by the leakage current of the SCs. The leakage current density of SCs-C was 62.5 μA/cm^2 at -1 V reverse bias, which is larger than that of SCs-A (1.3 μA/cm^2) or SCs-B (3.8 μA/cm^2). According to the leakage current of the SCs, SCs-B also exhibited a very high crystal quality as SCs-A. Given the significant reduction in V_{OC} of SCs, the conversion efficiency of SCs-B (3.74%) or SCs-C (3.28%) did not exceed that of SCs-A (4.44%).

To suppress the recombination centers and recover V_{OC} of the SCs with Ge QDs, the temperature-dependent V_{OC} was measured with a white light source. The temperature-dependent V_{OC} values of the three SCs are shown in Fig. 4(a). From 40 °C to −40 °C, the increases of V_{OC} were 0.131, 0.127, and 0.22 V, respectively. V_{OC} increased because of two main reasons: first, the broadened bandgap and increased quasi-Fermi level difference at low temperature,[27,28] and second, the suppression of recombination centers and longer carrier lifetime at low temperature. The temperature dependence of the bandgap energy of Si is expressed by[27]

$$\Delta E_g/\Delta T = -7.021 \times 10^{-4}\{1 - [1108/(1108 + T)]^2\} eV/K. \quad (1)$$

According to Eq. (1), the bandgap energy difference of bulk Si between 40 °C and −40 °C is 20 meV. According to the Fermi-Dirac distribution, the quasi-Fermi level difference between 40 °C and −40 °C is about 15 meV. Thus, they are not the main reasons for the recovery of V_{OC}. The V_{OC} of ideal diode is expressed by[28]

$$V_{OC} = \frac{kT}{q}\ln\left(\frac{I_P}{I_L} + 1\right), \quad (2)$$

where I_P is the photocurrent, and I_L is the leakage current. Temperature-dependent I_L of SCs-A and SCs-B slightly changed. A quasi-linear relationship between V_{OC} and temperature was observed. The slope and the increase in V_{OC} in SCs-B were almost similar to those in SCs-A. Thus, the V_{OC}

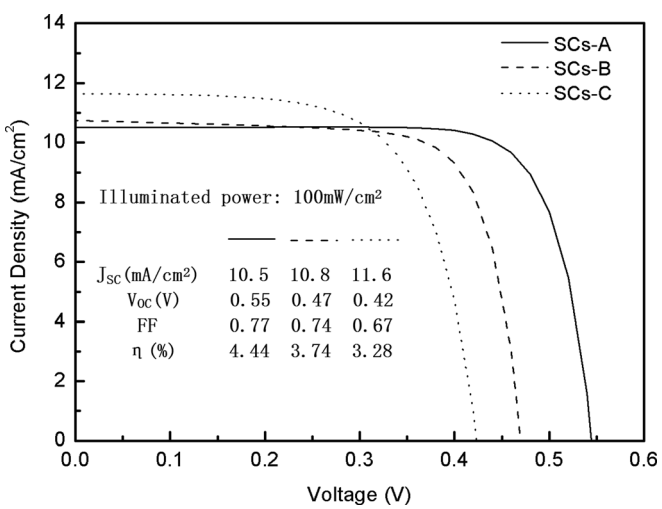

FIG. 3. I–V characteristics of the three SCs under standard illumination at room temperature. The illuminated power of the standard solar simulator is 100 mW/cm^2. J_{SC}, V_{OC}, FF, and efficiency of SCs are shown.

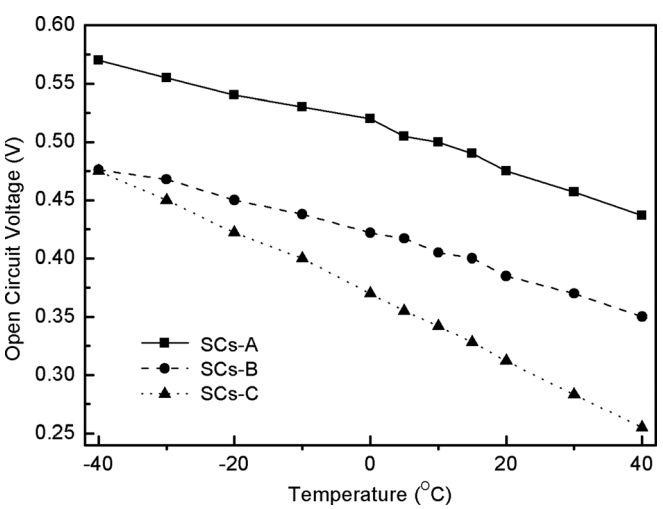

FIG. 4. Temperature-dependent V_{OC} of the three SCs. A quasi-linear relationship exists between V_{OC} and temperature. Compared with SCs-A and SCs-B, SCs-C has the highest V_{OC} recovery at low temperature.

recoveries in SCs-B and SCs-A were caused by the same factor. This phenomenon also indicates that SCs-B had high crystal quality. However, the I_L values of SCs-C were 120 and 16 μA/cm^2 at 40 °C and −40 °C, respectively. This notable behavior indicates that more recombination centers in SCs-C were suppressed at low temperature, which resulted in the highest V_{OC} recovery.

In summary, the SCs with 30 bilayers undoped or p-type Ge/Si QDs were fabricated on n^+-Si(001) substrates by UHV-CVD. Compared with SCs without Ge QDs, SCs with Ge QDs can enhance the photons absorption in the infrared region. Doping-induced defects can significantly decrease V_{OC} of SCs with Ge QDs. However, p-type doping is beneficial for the half-filling of Ge QDs levels and photo-carrier transfer of Ge QDs. The reduction in V_{OC} of SCs with Ge QDs induced by defects can recover significantly at low temperature. An optimized p-doping concentration can balance the defect density and photo-carrier transfer in SCs with Ge QDs. These results indicate that SCs with Ge QDs are potential candidates for high-efficiency SCs.

This work was supported by the National Natural Science Foundation of China (Grant Nos. 51072194, 61021003, 61036001, 61036003, 61176013, and 61177038).

[1]T. Trupke, M. A. Green, and P. Wurfel, J. Appl. Phys. **92**(7), 4117–4122 (2002).
[2]V. Aroutiounian, S. Petrosyan, A. Khachatryan, and K. Touryan, J. Appl. Phys. **89**(4), 2268–2271 (2001).
[3]K. A. Sablon, J. W. Little, V. Mitin, A. Sergeev, N. Vagidov, and K. Reinhardt, Nano Lett. **11**(6), 2311–2317 (2011).
[4]A. Luque and A. MartÃ, Adv. Mater. **22**(2), 160–174 (2010).
[5]A. Luque, P. G. Linares, E. Antolín, I. Ramiro, C. D. Farmer, E. Hernández, I. Tobías, C. R. Stanley, and A. Martí, J. Appl. Phys. **111**(4), 044502 (2012).
[6]S. M. Hubbard, C. D. Cress, C. G. Bailey, R. P. Raffaelle, S. G. Bailey, and D. M. Wilt, Appl. Phys. Lett. **92**(12), 123512 (2008).
[7]R. Oshima, A. Takata, and Y. Okada, Appl. Phys. Lett. **93**(8), 083111 (2008).
[8]D. Guimard, R. Morihara, D. Bordel, K. Tanabe, Y. Wakayama, M. Nishioka, and Y. Arakawa, Appl. Phys. Lett. **96**(20), 203507 (2010).
[9]A. M. Kechiantz, L. M. Kocharyan, and H. M. Kechiyants, Nanotechnology **18**(40), 405401 (2007).
[10]S. Fukatsu, H. Sunamura, Y. Shiraki, and S. Komiyama, Appl. Phys. Lett. **71**(2), 258–260 (1997).
[11]T. Tayagaki, N. Usami, W. Pan, Y. Hoshi, K. Ooi, and Y. Kanemitsu, Appl. Phys. Lett. **101**(13), 133905 (2012).
[12]M. K. Zundel, P. Specht, K. Eberl, N. Y. Jin-Phillipp, and F. Phillipp, Appl. Phys. Lett. **71**(20), 2972–2974 (1997).
[13]G. S. Solomon, J. A. Trezza, A. F. Marshall, and J. S. Harris, Phys. Rev. Lett. **76**(6), 952–955 (1996).
[14]H. M. Tawancy, Scr. Mater. **65**(10), 863–866 (2011).
[15]N. Usami, A. Alguno, K. Sawano, T. Ujihara, K. Fujiwara, G. Sazaki, Y. Shiraki, and K. Nakajima, Thin Solid Films **451–452**, 604–607 (2004).
[16]A. Alguno, N. Usami, T. Ujihara, K. Fujiwara, G. Sazaki, K. Nakajima, and Y. Shiraki, Appl. Phys. Lett. **83**(6), 1258–1260 (2003).
[17]N. Rappaport, E. Finkman, T. Brunhes, P. Boucaud, S. Sauvage, N. Yam, V. Le Thanh, and D. Bouchier, Appl. Phys. Lett. **77**(20), 3224–3226 (2000).
[18]A. I. Yakimov, V. A. Timofeev, A. A. Bloshkin, V. V. Kirienko, A. I. Nikiforov, and A. V. Dvurechenskii, J. Appl. Phys. **112**(3), 034511 (2012).
[19]P. Palacios, I. Aguilera, K. Sánchez, J. C. Conesa, and P. Wahnón, Phys. Rev. Lett. **101**(4), 046403 (2008).
[20]X. C. Liu and D. R. Leadley, J. Phys. D: Appl. Phys. **43**(50), 505303 (2010).
[21]M. Meduňa, O. Caha, M. Keplinger, J. Stangl, G. Bauer, G. Mussler, and D. Grützmacher, Phys. Status Solidi A **206**(8), 1775–1779 (2009).
[22]S. Das, K. Das, R. Singha, S. Manna, A. Dhar, S. Ray, and A. Raychaudhuri, Nanoscale Res. Lett. **6**(1), 416 (2011).
[23]Z. Liu, W. Hu, S. Su, C. Li, C. Li, C. Xue, Y. Li, Y. Zuo, B. Cheng, and Q. Wang, Opt. Express **20**(20), 22327–22333 (2012).
[24]Z. Liu, B. Cheng, W. Hu, S. Su, C. Li, and Q. Wang, Nanoscale Res. Lett. **7**(1), 383 (2012).
[25]V. S. Lysenko, Y. V. Gomeniuk, V. V. Strelchuk, A. S. Nikolenko, S. V. Kondratenko, Y. N. Kozyrev, M. Y. Rubezhanska, and C. Teichert, Phys. Rev. B **84**(11), 115425 (2011).
[26]K. Drozdowicz-Tomsia, E. M. Goldys, L. Fu, and C. Jagadish, Appl. Phys. Lett. **89**(11), 113510 (2006).
[27]Y. P. Varshni, Physica **34**(1), 149–154 (1967).
[28]S. M. Sze and K. K. Ng, *Physics of Semiconductor Devices* (Wiley-Interscience, 2006).